Electronic Properties of $AgBiS_2$ Nanocrystal Structure Variations

Yuta Tanaka[1], Fidya Azahro Nur Mawaddah[1], Dadan Suhendar[1], Satria Zulkarnaen Bisri[1]*

Department of Applied Physics and Chemical Engineering, Tokyo University of Agriculture and Technology, Tokyo, Japan
satria-bisri@go.tuat.ac.jp

Abstract. Today, most of the nanocrystals researched for use in electronic devices, such as solar cells and photodetectors, worldwide include toxic metal elements (Pb, Cd, or Hg) or scarce elements. To replace them with eco-friendly compounds, it is necessary to understand their electronic and optical properties to support their high performance. $AgBiS_2$, a promising ternary compound for environmental applications, is expected to be utilized in realizing solution-processed solar cells with high performance in terms of conversion efficiency. Same as PbS, $AgBiS_2$ has a NaCl-type cubic structure, but with two different cations (Ag or Bi). The order of these ions makes a difference in their structural and electronic properties. However, it is challenging to measure the details of the cation order experimentally. Therefore, a computational approach is crucial for investigating nanoscale properties. Here, we performed first-principles calculations using density functional theory (DFT) for one of the $AgBiS_2$ bulk crystalline structure phases, with a body-centered tetragonal (*bct*) primitive cell, and compared the results with those of the reported synthesized $AgBiS_2$ bulk crystal. The computed lattice constants are in close agreement with the experimental value. However, the electronic band structure has a small direct band gap of 0.07 eV, as determined by the PBE functional. In comparison with other phases, it is evident that cation order significantly affects the electronic properties.

Keywords: Nanocrystals, $AgBiS_2$, electronic band structure, DFT calculation.

1 Introduction

Nowadays, the performance of electronic devices has been increasing significantly due to ongoing research on materials and devices worldwide, which aims to address humanity's demands, including energy problems. For example, it is expected that solar cells incorporating nanomaterials, such as quantum dots, will exhibit good performance, surpassing the state-of-the-art silicon technologies. As of 2024, a solar cell with organic cation perovskite-based quantum dots has demonstrated a power conversion efficiency of 18.1% [1]. However, there are still many unoptimized uses of the unique features of the quantum dots. Quantum dots enable us to tune the band gap value by changing their size. The quantum confinement effect is responsible for this

S. C. Asih et al. (eds.), *Proceedings of the 19th International Conference on Quality in Research (QiR 2025)*, Advances in Engineering Research 303,
https://doi.org/10.2991/978-94-6239-717-0_14

feature. The full utilization of these features to demonstrate high-performance solar cells is currently underway. However, most of the researched nanocrystals for these applications contain toxic metal elements, such as Pb, Cd, or Hg. Furthermore, Se and Te, which are mainstream for studying metal chalcogenide nanocrystals, are scarce on Earth and challenging to find. Therefore, we need to find better alternatives than these nanocrystal compounds.

The ternary compound $AgBiS_2$ is a promising material for eco-friendly optoelectronic devices, including solar cells. [2] According to experimental reports, the band gap of this compound is approximately 0.9 eV in its bulk crystal form. [3] If the quantum confinement effect can be strongly controlled in the nanocrystal form of this compound, the band gap value can be enlarged. However, due to the present challenge of size limitation, the obtained band gap of $AgBiS_2$ nanocrystals can only be enlarged up to 1.1 – 1.3 eV, which is not significantly different from its bulk value. [2][4][5][6][7] Nevertheless, these bandgap values are within the ideal wavelength range for solar cell operation, comparable to those of silicon and PbS quantum dots.

There are two types of $AgBiS_2$: schapbachite and matildite. Recently, we synthesized $AgBiS_2$ nanocrystals that exhibited semiconducting behavior and were confirmed to be schapbachite $AgBiS_2$. [8]Same as cubic PbS, schapbachite $AgBiS_2$ has a NaCl-like cubic structure and space group $Fm\bar{3}m$ with two cations (Ag and Bi) and one anion (S). Therefore, there are many possibilities of crystalline structure depending on the cation order. On the other hand, matildite $AgBiS_2$ has a trigonal structure and space group $P\bar{3}m1$. [9] Two of the possible crystalline structures with VESTA [10] are shown in Fig. 1(a-b). Bulk $AgBiS_2$ crystallizes in a trigonal structure at room temperature and transforms to a cation-disordered cubic structure. [11]

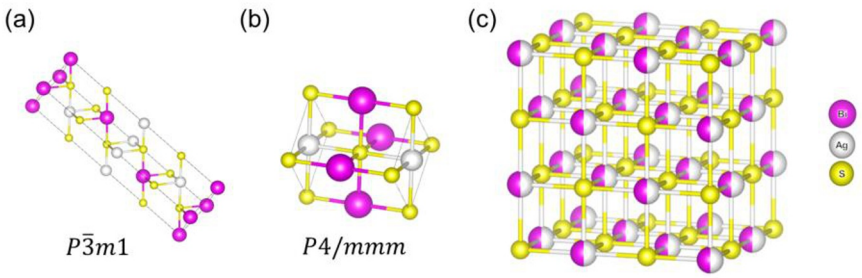

Fig. 1. Two of the variations of $AgBiS_2$ primitive cells: (a) trigonal $P\bar{3}m1$, and (b) tetragonal $P4/mmm$. (c) The cubic supercell includes 64 atoms

Although the cation order influences the structural and electronic properties, it is difficult to investigate the cation order experimentally. Therefore, computational calculations are crucial in explaining the cation order, which can serve as a guideline for designing related experiments.

There have been reports on the theoretical calculation study of $AgBiS_2$, and many of them have departed from various possible crystalline structures. For instance, some reports indicated that $AgBiS_2$ with a tetragonal structure (space group: $P4/mmm$) has no band gap, [12][13][14] suggesting this compound is not a semiconductor. On the

other hand, Mehdaoui et al. [15] indicated that $AgBiS_2$ with $P\bar{3}m1$ structure has less total energy than $AgBiS_2$ with $P4/mmm$ structure, suggesting that the $P\bar{3}m1$ structure is more stable. Other researchers have attempted to calculate variations in other crystal structures. [12][16][17] It was reported that ion order might be important. Some calculations revealed that the Ag-S-Ag-S chain contributes to the valence band maximum, and the Bi-S-Bi-S chain contributes to the conduction band minimum. [12] Considering cation disorder, cubic unit supercells are usually used for calculations, as shown in Fig. 1(c). The supercell in Fig. 1(c) contains 32 S, 16 Ag, and Bi atoms as an example. Even in this case, the number of combinations of Ag and Bi is $32!/(16!)^2$ without considering symmetry. [13]

The prospect of this compound demonstrating a solar cell with high power conversion efficiency has been conceptually predicted, suggesting that an ultra-thin film of $AgBiS_2$ may achieve a high-power conversion efficiency (PCE) of 25%. [18] However, to date, the reported efficiency of $AgBiS_2$ thin-film solar cells is still around 9-10%. Therefore, to fabricate ideal solar cells, it is necessary to understand the optical and electronic properties, especially the intrinsic properties of the materials.

Here, we report the results of a computational study on the electronic properties of the $AgBiS_2$ crystal structure with body-centered tetragonal (*bct*) structure (space group $I4_1/amd$). Although $I4_1/amd$ $AgBiS_2$ has less total energy than $P4/mmm$ $AgBiS_2$ theoretically, there are less researches for $I4_1/amd$ $AgBiS_2$ than $P4/mmm$ $AgBiS_2$. [16] In this study, we performed first-principles calculations to investigate the electronic band structures of $AgBiS_2$ using two kinds of approximations. Understanding the electronic band structures of this compound will enable us to predict whether variations in its structure will lead to the formation of metal, semiconductor, or insulator behaviors (Fig. 2). [19]

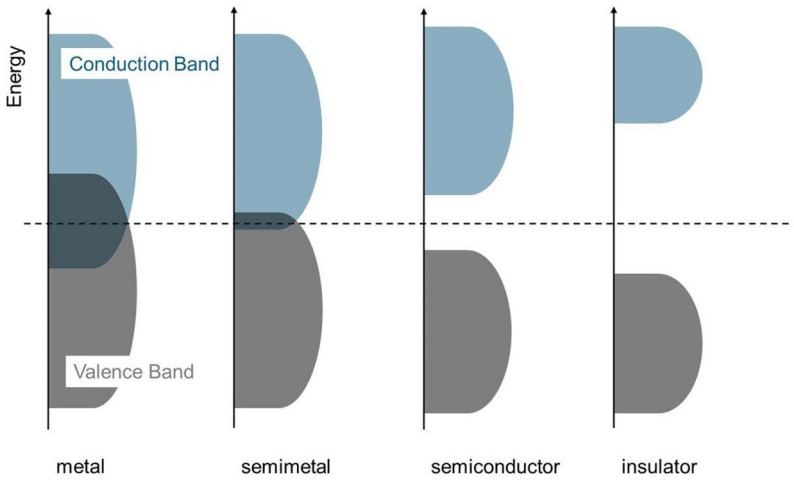

Fig. 2. The illustration of the electronic band diagram for each type of material: metal, semimetal, semiconductor, and insulator. [19]

Metallic materials have their Fermi level in the conduction band, resulting in a high density of free electrons, and their conduction band and valence band overlap in many cases. In contrast, semiconductors and insulators exhibit areas where there are no allowed electronic energy states between their conduction bands and valence bands, which is manifested as the electronic band gap.

2 Materials and Methods

2.1 Materials

In this study, we focus on one of the schapbachite $AgBiS_2$ crystalline structure phases: body-centered tetragonal (*bct*) structure with space group $I4_1/amd$. The primitive cell is shown in Fig. 3. This phase was introduced by Ju et al. [12] as the AF-III primitive cell. For the calculation performed in this study, the unit cell used is a tetragonal structure, serving as an approximation to the *bct* structure.

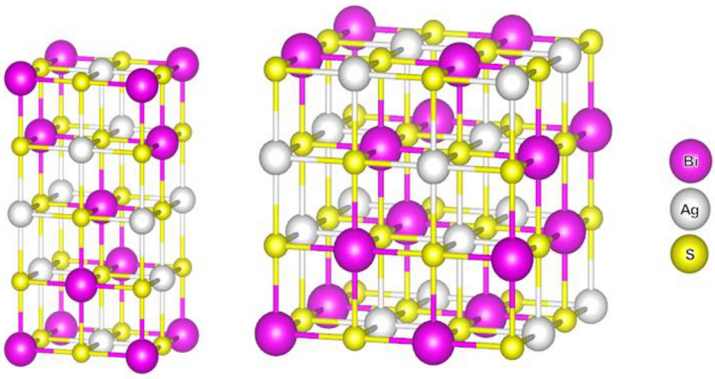

Fig. 3. (left)The primitive cell and (right)the supercell (with 64 atoms) of $AgBiS_2$ $I4_1/amd$ structure.

2.2 Methods

First-principles calculations were performed using Density Functional Theory (DFT) within the Quantum ESPRESSO [20][21][22] package. In this study, a full-relativistic pseudopotential is used in conjunction with the PBE [23] and LDA [24] exchange–correlation (*xc*) functionals. PBE is one of the generalized gradient approximation (GGA) forms [25]. LDA is the simplest approximation form for the *xc* functional that considers the electron density. GGA introduces a dependence on the electron density gradient. All calculations were performed using an energy cutoff of 45.0 Ry. For electron–electron interaction, the projected augmented wave (PAW) method [26][27] is used.

3 Results

The appropriate lattice constants of $AgBiS_2$ were investigated. The computed lattice constants are shown in Table 1. The lattice constant *a* in the primitive cell is compatible with that in the cubic structure, and these are similar to twice the length of the Ag-S or Bi-S chains. The computed values with the PBE functional are in good agreement with a reference journal,[16] where all-electron calculations with the PBE functional were carried out. The experimental lattice constants for the cubic structure (with cation order not identified) were obtained at 5.651 Å from references for comparison. [28] [29]

Table 1. The computed lattice parameters.

Parameter	PBE	LDA	Ref. (PBE) [16]	Expt. [28] [29]
Lattice constant *a* [Å]	5.637	5.516	5.70	5.651
Lattice constant *c* [Å]	11.44	10.88	11.45	–
c/a	2.030	1.972	2.01	–
Unit cell volume *V* [Å^3]	363.7	330.9	372.0	–

To understand the electronic properties of bulk $AgBiS_2$, we performed the band calculations. The electronic band structures for bulk $AgBiS_2$ with $I4_1/amd$ structure at the PBE and LDA levels are shown in Fig. 4. The horizontal axis represents the high symmetry k-points in the Brillouin zone. [30]

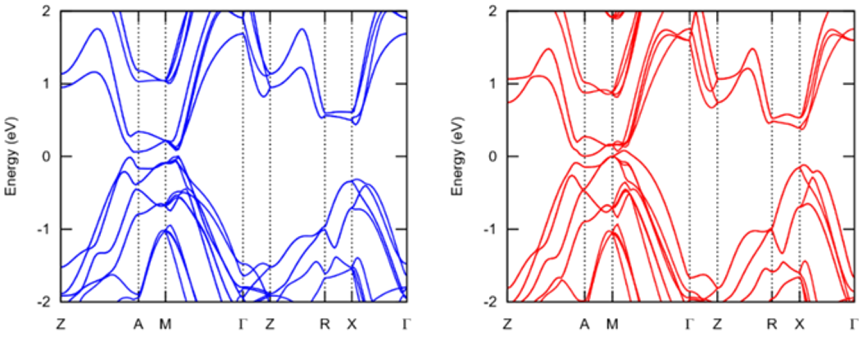

Fig. 4. The electronic band structures at the (left) PBE and (right) LDA level.

For the band structure with the PBE functional, a small direct band gap of 0.07 eV is obtained. This band gap value is close to the reference value (0.05 eV). [16] On the other hand, there is no band gap in the band structure obtained from the calculation using the LDA functional.

4 Discussion

Although the band structure exhibits a band gap with the PBE functional (0.07 eV), this value is significantly smaller than the experimental result (0.9 eV). [8] From this difference, it is suggested that $I4_1/amd$ structure phase is not the experimentally synthesized $AgBiS_2$.

For other structure phases, matildite $AgBiS_2$ ($P\bar{3}m1$) has an indirect band gap of 0.42 eV within the PBE functional.[14] Also, as mentioned above, $P4/mmm$ structure phase has no band gap [12][13][14]. One thing to consider is that LDA and GGA tend to underestimate the band gap value generally.

Experimentally, the reported band gap values of $AgBiS_2$ are various. This band gap difference may be dependent not only on nanocrystal sizes, but also on the cation order. For example, $AgBiS_2$ quantum dots synthesized by two groups have a band gap of 1.10 eV for 4.2 nm size [6] and of 1.3 eV for 4.62 ± 0.97 nm size [2]. These crystals were synthesized using various methods [31], resulting in different cation orders, crystal shapes, and so on.

5 Conclusion

We have performed the computational study for $AgBiS_2$ bulk with $I4_1/amd$ structure phase. The electronic band structure has a band gap of 0.07 eV for the PBE level and no band gap for the LDA level. This value is far smaller than the experimentally obtained band gap of 0.9 eV. Furthermore, according to reports from other researchers, other cation order phases have different band gap values theoretically. These results indicate that cation order has a strong influence on electronic properties. Controlling the cation order is crucial for making $AgBiS_2$ nanocrystals into a building block for solar cells with improved performance and other optoelectronic and energy device applications.

Acknowledgments. This research was partly supported by the 2023 Iketani Science and Technology Foundation Research Grant (grant number 0351125-A) and the 2024 Thermal & Electric Energy Technology Foundation Research Grant. Y.T. acknowledges support from the Tokyo University of Agriculture and Technology International Affairs Office.

Disclosure of Interests. The authors declare no conflicts of interest.

References

1. Aqoma H, Lee S-H, Imran I F, Hwang J-H, Lee S-H, Jang S-Y. Alkyl ammonium iodide-based ligand exchange strategy for high-efficiency organic-cation perovskite quantum dot solar cells. Nat. Energy 2024, 9, 324–332. https://doi.org/10.1038/s41560-024-01450-9
2. Bernechea M, Cates N, Xercavins G, So D, Stavrinadis A, Konstantatos G. Solution-processed solar cells based on environmentally friendly $AgBiS_2$ nanocrystals. Nat. Photon. 2016, 10, 521–525. https://doi.org/10.1038/nphoton.2016.108
3. Golovach I I, Gerasimenko V S, Slivka V Y, Dovgoshei N I, Golovei M I, Bogdanova A V. Vitrification of and optical and photoelectrical properties of $AgAsS_2$, $AgSbS_2$, and $AgBiS_2$. Izv. Vyssh. Uchebn. Zaved. Fiz. 1976, 3, 39.
4. Pejova B, Nesheva D, Aneva Z, Petrova A. Photoconductivity and Relaxation Dynamics in Sonochemically Synthesized Assemblies of $AgBiS_2$ Quantum Dots. J. Phys. Chem. C 2011, 115, 1, 37–46. https://doi.org/10.1021/jp106605t
5. Huang P-C, Yang W-C, Lee M-W. $AgBiS_2$ Semiconductor-Sensitized Solar Cells. J. Phys. Chem. C 2013, 117, 36, 18308–18314. https://doi.org/10.1021/jp4046337
6. Pejova B, Grozdanov I, Nesheva D, Petrova A. Size-Dependent Properties of Sonochemically Synthesized Three-Dimensional Arrays of Close-Packed Semiconducting $AgBiS_2$ Quantum Dots. Chem. Mater. 2008, 20, 7, 2551–2565. https://doi.org/10.1021/cm071794k
7. Nesheva D, Aneva Z, Pejova B, Grozdanov I, Petrova A. Photoelectrical characterization of nanocrystalline $AgBiS_2$ thin films, J. Optoelectron. Adv. M. 2009, 11(9), 1347-1350.
8. Mawaddah F A N, Suhendar D, Tanaka Y, Kitada K, Shimizu T, Minoda H, Bisri S Z. Evolution of the formation of $AgBiS_2$ colloidal nanocrystals for optoelectronic devices. Nanoscale 2025. Advanced article. https://doi.org/10.1039/D5NR01707F
9. Viñes F, Konstantatos G, Illas F. Matildite Contact with Media: First-Principles Study of AgBiS Surfaces and Nanoparticle Morphology. J. Phys. Chem. B 2018, 122, 2, 521–526.
10. Momma K, Izumi F. VESTA: a three-dimensional visualization system for electronic and structural analysis. J. Appl. Cryst. 2008, 41(3), 653-658. https://doi.org/10.1107/S0021889808012016
11. Guin S N, Banerjee S, Sanyal D, Pati S K, Biswas K. Origin of the Order-Disorder Transition and the Associated Anomalous Change of Thermopower in $AgBiS_2$ Nanocrystals: A Combined Experimental and Theoretical Study. Inorg Chem. 2016, 55(12), 6323-31. 10.1021/acs.inorgchem.6b00997.
12. Ju M-G, Dai J, Ma L, Zhou Y, Zeng X C. $AgBiS_2$ as a low-cost and eco-friendly all-inorganic photovoltaic material: nanoscale morphology–property relationship. Nanoscale Adv. 2020, 2(2), 770-776. http://dx.doi.org/10.1039/C9NA00505F
13. Viñes F, Konstantatos G, Illas F. Bandgap engineering by cationic disorder: case study on $AgBiS_2$. Phys. Chem. Chem. Phys., 2017,19, 27940-27944. https://doi.org/10.1039/C7CP05118B
14. Viñes F, Bernechea M, Konstantatos G, Illas F. Matildite versus schapbachite: First-principles investigation of the origin of photoactivity in $AgBiS_2$. Phys. Rev. B 2016, 94, 235203
15. Mehdaoui L, Miloua R, Khadraoui M, Bensaid M O, Abdelkader D, Chiker F, Bouzidi A. Theoretical analysis of electronic, optical, photovoltaic and thermoelectric properties of $AgBiS_2$. Physica B: Condensed Matter 2019, 564, 114-124. https://doi.org/10.1016/j.physb.2019.04.006
16. Suzuki S, Tsuyama M. Theoretical study of structural, electronic, and optical properties of ternary metal sulfides $MBiS_2$ (M = Ag, Na). Jpn. J. Appl. Phys. 2020, 59, 041002.

17. Koskela K M, Pakhira A, Strumolo M J, Banerjee S, Brutchey R L. Interplay between Cation "Coloring" and Stereochemically Active Lone Pairs in $AgBiS_2$ Thin Films. Inorg. Chem. 2025, 64, 20, 10097–10105. https://doi.org/10.1021/acs.inorgchem.5c00710
18. Wang Y, Kavanagh S R, Burgués-Ceballos I, Walsh A, Scanlon D O, Konstantatos G. Cation disorder engineering yields $AgBiS_2$ nanocrystals with enhanced optical absorption for efficient ultrathin solar cells. Nat. Photon. 2022, 16, 235-241. https://doi.org/10.1038/s41566-021-00950-4
19. Tanaka Y, Computational Study for New 2D Iron Sulfide by First-Principles Calculation, Graduation Thesis, Department of Applied Physics and Chemical Engineering, Tokyo University of Agriculture and Technology, Japan, 2025.
20. Giannozzi P, Baroni S, Bonini N, Calandra M, Car R, Cavazzoni C, et al. QUANTUM ESPRESSO: a modular and open-source software project for quantum simulations of materials. J. Phys.: Condens. Matter 2009, 21(39), 395502.
21. Giannozzi P, Andreussi O, Brumme T, Bunau O, Nardelli M B, Calandra M, et al. Advanced capabilities for materials modelling with Quantum ESPRESSO. J. Phys.: Condens. Matter 2017, 29(46), 465901.
22. Giannozzi P, Baseggio O, Bonfà P, Brunato D, Car R, Carnimeo I, et al. Quantum ESPRESSO toward the exascale. J. Chem. Phys. 2020, 152(15), 154105.
23. Perdew J P, Ruzsinszky A, Csonka G I, Vydrov O A, Scuseria G E, Constantin L A, et al. Restoring the Density-Gradient Expansion for Exchange in Solids and Surfaces. Phys. Rev. Lett. 2008, 100(13), 136406 ; Erratum Phys. Rev. Lett. 2009, 102(3), 039902.
24. Kohn W, Sham L J. Self-Consistent Equations Including Exchange and Correlation Effects. Phys. Rev. 1965, 140(4A), A1133.
25. Perdew J P, Chevary J A, Vosko S H, Jackson K A, Pederson M R, Singh D J, Fiolhais C. Atoms, molecules, solids, and surfaces: Applications of the generalized gradient approximation for exchange and correlation. Phys. Rev. B 1992, 46(11), 6671; Erratum Phys. Rev. B 1993, 48(7), 4978.
26. Blöchl P E. Projector augmented-wave method. Phys. Rev. B 1994, 50(24), 17953.
27. Kresse G, Joubert D. From ultrasoft pseudopotentials to the projector augmented-wave method. Phys. Rev. B 1999, 59(3), 1758.
28. Geller S, Wernick J H. Ternary semiconducting compounds with sodium chloride like structure: $AgSbSe_2$, $AgSbTe_2$, $AgBiS_2$, $AgBiSe_2$. Acta Crystallogr. 1959, 12, 46–54. https://doi.org/10.1107/S0365110X59000135.
29. Shen G, Chen D, Tang K, Qian Y. Novel polyol route to $AgBiS_2$ nanorods, J. Cryst. Growth 2003, 252, 199–201. https://doi.org/10.1016/S0022-0248(02)02500-9
30. Setyawan W, Curtarolo S. High-throughput electronic band structure calculations: Challenges and tools. Comput. Mater. Sci. 2010, 49(2), 299-312.
31. Mawaddah F A N, Bisri S Z. Advancing Silver Bismuth Sulfide Quantum Dots for Practical Solar Cell Applications. Nanomaterials 2024, 14(16), 1328. https://doi.org/10.3390/nano14161328